Available online at www.sciencedirect.com
ScienceDirect
Polymer 47 (2006) 6322–6327
polymer
www.elsevier.com/locate/polymer

Preparation of non-woven mats from all-aqueous silk fibroin solution with electrospinning method

Chen Chen, Cao Chuanbao*, Ma Xilan, Tang Yin, Zhu Hesun

Research Center of Material Science, Beijing Institute of Technology, No. 5, Zhongguancun South Street, Beijing 100081, China

Received 24 October 2005; received in revised form 2 July 2006; accepted 5 July 2006
Available online 26 July 2006

Abstract

In the present study, we successfully prepared non-woven mats from stable regenerated silk fibroin aqueous solution at high concentration. Scanning electronic microscope (SEM) was used to observe the morphology of the fibers. The structure of the fibers was characterized using Fourier transform infrared (FTIR), wide-angle X-ray diffraction (WAXD) and differential scanning calorimetry (DSC). The mechanical tests were also performed. In the as-spun fibers, silk fibroin was present in a random coil conformation, the stress and strain at break were 0.82 MPa and 0.76%, respectively, while after methanol treatment, the silk fibroin was transformed into a β-sheet-containing structure, the stress and strain at break increased to 1.49 MPa and 1.63%, respectively. This study provided an option for the electrospinning of silk fibroin without using organic solvent or blending with any other polymers, which may be important in tissue engineering scaffold preparation.

Keywords: Electrospinning; Aqueous solution; Silk fibroin

1. Introduction

In recent years, the electrospinning process has gained much attention because it is an effective method to manufacture ultrafine fibers or fibrous structures of many polymers with diameter in the range from several micrometers down to tens of nanometers [1–4]. In the electrospinning process, a high voltage is used to create an electrically charged jet of a polymer solution or a molten polymer. This jet is collected on a target as a non-woven fabric. Because these nanofibers have some useful properties such as high specific surface area and high porosity [1], they can be used as filters [5], wound dressings [6], tissue engineering scaffolds [7], etc.

Silk fibroin (SF) is the protein that forms filaments of silkworm silk and gives silk high mechanical strength, elasticity, and softness. In addition to the outstanding mechanical properties, silk fibroin displays good biological compatibility [8]. It has been demonstrated that silk fibroin-derived scaffolds may have wide-range applications in the fabrication of replacement tissue [9]. Electrospinning is a unique method capable of producing fibers from both synthetic and natural polymers for biomedical application [10], because electrospun non-woven fibers have high specific surface area and highly porous 3-D structure that are desirable for high-density cell and tissue cultures; electrospun non-woven fibers are among the most promising material forms used in various tissue engineering applications [1] and can be considered as ideal candidates [11], for example, Min et al. found that the SF nanofiber matrix can promote cell adhesion [12]. SF has been electrospun with the spinning solvents such as hexafluoro-2-propanol (HFIP) [13], hexafluoroacetone (HFA) [14] and formic acid [1,15] or in combination with PEO [16,17].

Organic solvents can pose problems when the processed materials are exposed to cells in vitro or in vivo; avoiding the use of organic solvents can enhance the potential biocompatibility of the electrospun fibers. To address this goal, Jin et al. reported that they conducted a process for silk electrospinning in combination with PEO [17]. In this study, we tried

* Corresponding author. Tel.: +86 10 6891 3792; fax: +86 10 6891 2001.
E-mail address: cbcao@bit.edu.cn (C. Chuanbao).

0032-3861/$ - see front matter © 2006 Elsevier Ltd. All rights reserved.
doi:10.1016/j.polymer.2006.07.009

to develop the SF electrospinning with two major purposes. First, we wanted to avoid the problem that derived from residual organic solvents when the SF fibers were exposed to cell in vitro or in vivo and improve the potential biocompatibility of the SF non-woven mats. To overcome this problem, water was used as electrospinning solvent. Second, to simplify the process of electrospinning, instead of blending with other materials, the concentrated solution that was appropriate for electrospinning was prepared by concentrating the SF solution. Thus, an all-aqueous process for SF electrospinning was developed and SF non-woven mats were fabricated.

2. Experiment

2.1. Preparation of regenerated Bombyx mori SF solution [18]

Raw silk was degummed with 0.5% (w/w) Na_2CO_3 solution at 100 °C for 60 min and then washed with distilled water. Degummed silk was dissolved in a ternay solvent system of $CaCl_2/H_2O$/EtOH solution (1/8/2 in mole ratio) for 40 min at 80 °C and dialyzed to remove salts in a cellulose tube against distilled water for 3 days at room temperature, then the SF solution was filtered.

2.2. Preparation of the spinning solution

The obtained solution was directly concentrated to generate about 28%, 30%, 32%, 34% and 37% SF solutions by weight with slow stirring at 50–60 °C. With the continuous stirring, the SF solution was prevented from turning into gel during the concentrating process. The viscosity of the solutions was measured with a viscometer (NDJ-1, Shanghai Precision & Scientific Instrument Co., Ltd) at room temperature.

2.3. Electrospinning

In the electrospinning process, the capillary with axis tilted about 45° from horizontal direction was connected to a syringe filled with 5 ml SF solution. A high voltage in the range from 12 kV to 20 kV was applied to the droplet of SF solution at the tip. A grounded aluminum foil was placed at a distance of 18 cm from the capillary tip.

2.4. Treatment of electrospun mats

As-spun SF mats were immersed into a 90/10 (v/v) methanol/water solution for 10 min and then dried under vacuum at room temperature for 24 h.

2.5. Characterization

The morphology of the electrospun fibers was observed with a scanning electronic microscope (SEM) (S-3500, HITACHI). Infrared spectra were measured with an attenuated total reflectance accessory (ATR) (FTS 3100, DIGILAB), each spectrum was acquired in transmittance mode on a ZnSe crystal by accumulation of 16 scans with a resolution of 4 cm^{-1} and a spectral range of 4000–600 cm^{-1}. Wide-angle X-ray diffraction (WAXD) curves were recorded with an X-ray diffractometer (X'pertproMPD, PaNalytical) with X'celerator counter at a scanning rate of 0.066°/min and within the scanning region of $2\theta = 5–40°$, with Cu K_α radiation ($\lambda = 1.5418$ Å), irradiation conditions were 40 kV and 40 mA. The thermographs were acquired using a differential scanning calorimeter (DSC-60, Shimadzu) from room temperature to 300 °C at the rate of 10 °C/min under a nitrogen atmosphere. The mechanical properties of specimens (15×50 mm^2) were obtained using a testing machine (3365, Instron) under ambient condition, the thickness of the samples was from 0.17 mm to 0.33 mm, gauge length was set at 30 mm and the rate of the crosshead was 1 mm/min.

3. Results and discussion

3.1. Stability of the SF solution

Viscosity plays an important role in the electrospinning process. The jet from low viscosity liquids breaks up into droplets more readily and few fibers are formed, while at high viscosity, electrospinning is prohibited because of the instability of flow caused by the high cohesiveness of the solution. To the SF aqueous solution electrospinning, the former is the primary problem. Increasing the concentration of the SF solutions to acquire SF solutions which are of enough viscosity is a direct and simple method, but gel formation of SF solutions occurs at high concentration. It is true that the gelation time for the SF solution decreases with increasing concentration; however, it is possible that the SF aqueous solution with high concentration can be of good stability, for instance, the concentration of SF solution can reach up to 30% in the gland of the silkworm; for the SF/water system studied here, the gelation time is 4 days at 25 °C when the concentration is 37% (w/w), which is stable enough to be used in electrospinning.

3.2. Morphology under different viscosity and voltage

In electrospinning, the morphology of the electrospun products varied with concentration of the SF solutions. Fig. 1 showed the variation in viscosity with the concentration of SF solutions. At concentration above 30% (w/w), the viscosity increased dramatically, which indicated that there were extensive chain entanglements at this concentration [1].

The SEM micrographs of electrospun fibers from SF solutions with different concentrations or viscosities, ranging from about 28% (w/w) to about 37% (w/w) and from SF solutions with a concentration of 34% (w/w) at a series of voltage from 12 kV to 20 kV, were shown in Figs. 2 and 3, respectively. SEM photographs showed that the SF fibers deposited randomly and the thickness was from 500 nm to 10 μm. SF fibers intersected each other to make up numerous pores, whose size reached up to several tens of microns, which made the SF non-woven mats to have a very porous structure. As shown in Fig. 2, at concentration of 28% (w/w) (Fig. 2(a)), fibers

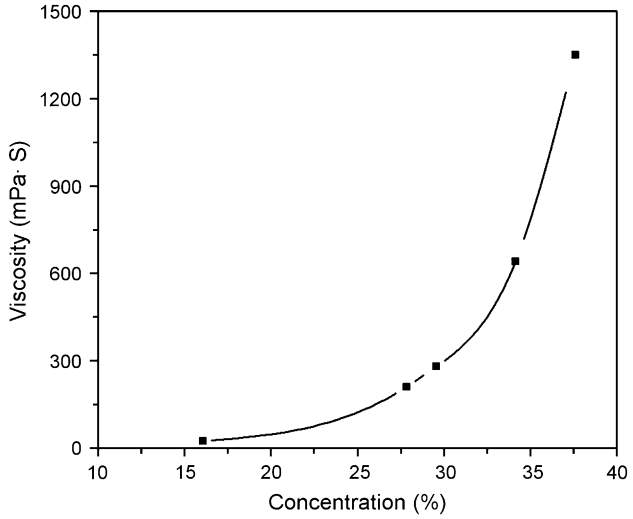

Fig. 1. Variation in viscosity with the concentration of SF aqueous solution.

together with droplets and beaded fibers were observed; at a higher concentration of 32% (w/w), droplets disappeared and the beaded fibers became fewer; no droplets or beaded fibers were observed at the concentration of 34% (w/w) or 37% (w/w). Since jet breakup depends on viscosity [19,20], based on the relationship between concentration and viscosity shown in Fig. 1, the jet with a low concentration broke into droplets readily and a mixture of fibers, bead fibers and droplets as a result of low viscosity was generated, fibers had an irregular morphology with large variation in size, while jet with high concentration didn't break up but traveled to the grounded target and tended to facilitate the formation of fibers without beads and the decrease of droplets for high viscosity, fibers became more uniform and had regular morphology. However, there was a high concentration end because the solution with concentration of about 37% (w/w) was proved difficult to flow through the syringe needle of the apparatus and the droplet of solution suspended at the end of the syringe needle dried

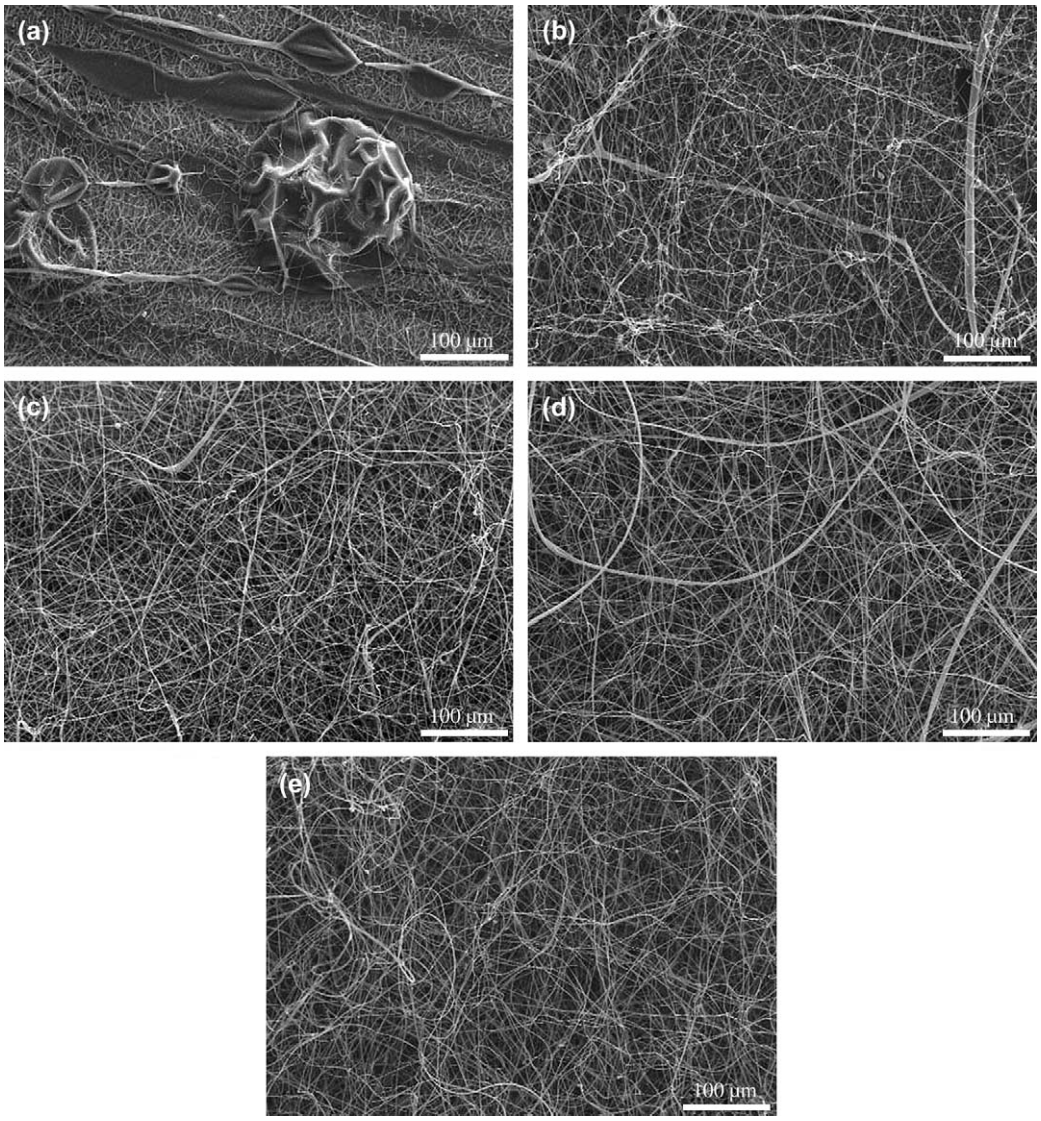

Fig. 2. The morphology of fibers at the voltage of 20 kV at concentration of (a) 28%, (b) 30%, (c) 32%, (d) 34%, (e) 37% with a constant spinning distance of 18 cm (scale bar, 100 μm).

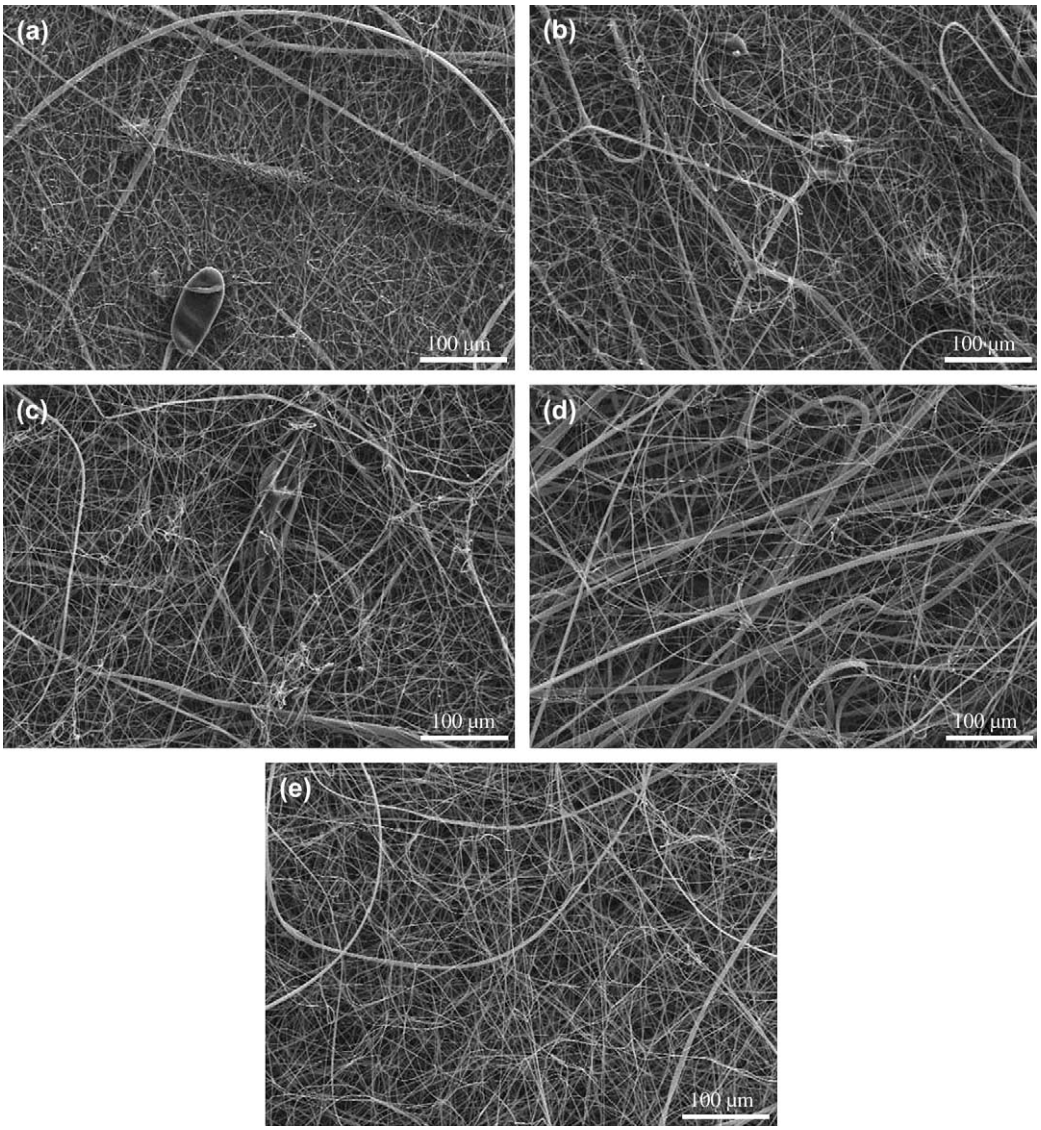

Fig. 3. The morphology of fibers at the concentration of 34% at voltage of (a) 12 kV, (b) 14 kV, (c) 16 kV, (d) 18 kV, (e) 20 kV with a constant spinning distance of 18 cm (scale bar, 100 μm).

readily in the electrospinning process. Fig. 3 showed the effects of the electrical field on the morphology of the fibers. In the experiments, the beads were found in the electrospun products when the applied voltage was not higher than 16 kV and there were few beads at the voltage of 18 kV or 20 kV. Because the distance was fixed, higher voltage resulted in a higher charge density on the surface of the solution jet during the electrospinning process. Like the addition of salt to the solution, that higher net charge density resulted from higher voltage on the jet also imposed higher elongation forces to the jet, which resulted in small beads and smooth fibers were produced [3]; however, further increasing voltage may decrease the stability of the initiating jet and the fibers became rough [19].

The solution with a concentration of 34% (w/w) was chosen to fabricate non-woven mats at the voltage of 20 kV with a spinning distance of 18 cm, the detailed morphology of fibers is shown in Fig. 4, the fibers had a belt-like morphology instead of general wire morphology. In fact, fibers in the products electrospun under all preparation conditions had the belt-like morphology in this study. Koombhongse et al. [21] considered that the belt-like morphology resulted from the presence of a thin, mechanically distinct polymer skin; in brief, after the skin formed, the solvent inside escaped, atmosphere pressure tended to collapse the tube formed by the skin as the solvent evaporated, the circular cross section became elliptical and then flat, forming a ribbon with a cross-sectional perimeter nearly the same as the perimeter of the jet. Therefore, this phenomenon may be a sign that indicated a skin was formed on the liquid jet.

3.3. The structure of the non-woven mats

Infrared spectroscopy (IR) had been often applied to study the molecular conformation of silk fibroin fibers or films. Random coil showed strong absorption bands at 1665 cm^{-1}

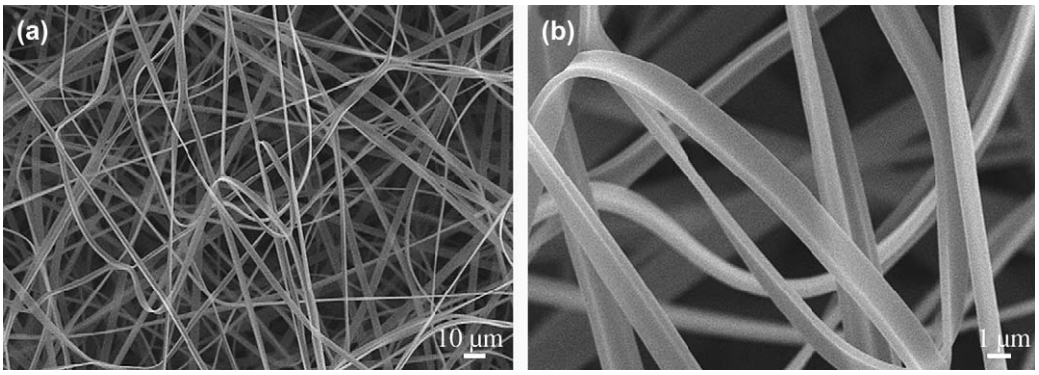

Fig. 4. SEM images of the electrospun fibers from the SF aqueous solution with a concentration of 34% at the voltage of 20 kV with a constant spinning distance of 18 cm: (a) ×1000 (scale bar, 10 μm), (b) ×5000 (scale bar, 1 μm).

(amid I), 1540 cm^{-1} (amid II) and 1235 cm^{-1} (amid III), while the β-sheet showed absorption bands at 1628 cm^{-1} (amid I), 1533 cm^{-1} (amid II) and 1265 cm^{-1} (amid III) [22]. As shown in Fig. 5, the structure of the as-spun mats was characterized by absorption bands at 1647 cm^{-1} (amid I) and 1535 cm^{-1} (amid II), attributed to the random coil or silk I; random coil form and silk I were not differentiated here because of the similarity between their infrared spectra [23]. On the contrary, the fibers showed strong β-sheet absorptions at 1626 cm^{-1} (amid I) and 1519 cm^{-1} (amid II) after methanol treatment. Fig. 6 showed the wide-angle X-ray diffraction (WAXD) patterns. The WAXD patterns of as-spun fibers exhibited only a broad peak centered at 22.8°, no groups of diffraction peaks characteristic of the crystalline β-sheet were found, which indicated that the SF was amorphous in the as-spun fibers. This result can be explained by the facts that the rapid evaporation of the solvent, the slow rate of crystallization for SF from water as well as the short travel time of the jet in air before depositing on the collecting device placed a limit on molecular rearrangement and crystallization, even though the elongation rate reached up to 10^6 times in a short distance in less than a minute [16]. After methanol treatment, a peak at 20.7° (crystalline spacing of 4.3 Å) was observed from WAXD, this peak was a characteristic of β-sheet structure [24–26]. WAXD data confirmed the conversion observed in FTIR that the structure transformed from predominantly random coil into predominantly β-sheets. The thermograms of the fibers are shown in Fig. 7. Both samples exhibited two big endothermic peaks around 100 °C and 280 °C. The former was attributed to evaporation of the water and the latter was attributed to the destruction of the SF. For the as-spun fibers, a small exothermic peak appeared at 228 °C, which indicated that a cold crystallization of β-crystallites from the random coil occurred [27]. For the methanol-treated fibers, no exothermic peak was observed till the sample was heated to degradation point. Though heat treatment can also induce conformational transitions, that the fibers after methanol treatment have a higher degradation temperature indicates that the thermal degradation temperature seems to be more affected by methanol treatment compared with the heat treatment. The thermo analysis results were consistent with the conclusions from FTIR and WAXD that the SF was uncrystallized in the as-spun fibers.

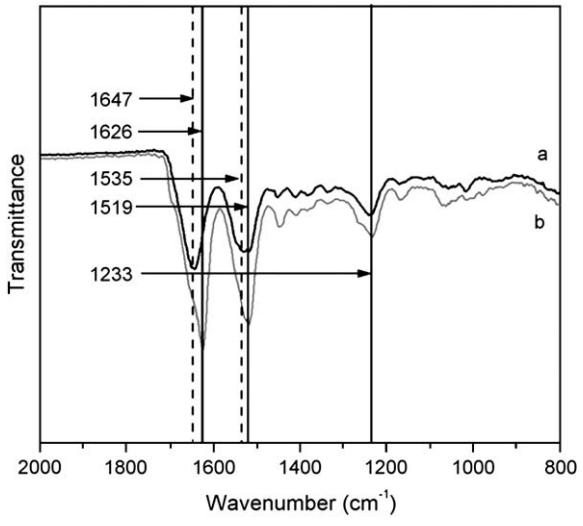

Fig. 5. FTIR-ATR spectra of electrospun fibers: (a) as-spun fibers, (b) methanol-treated fibers.

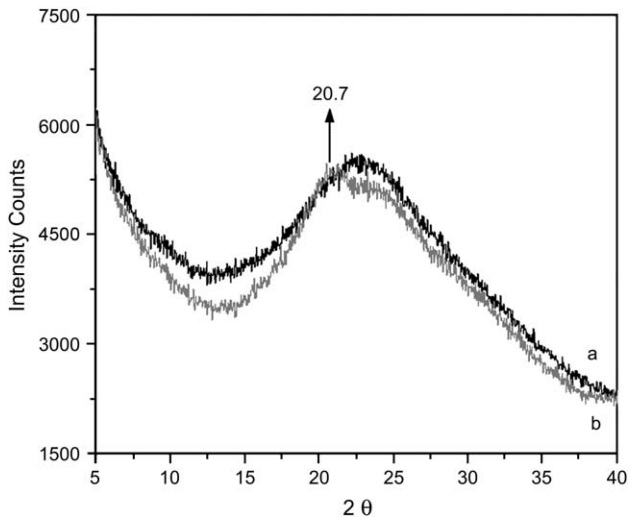

Fig. 6. WAXD of electrospun fibers: (a) as-spun fibers, (b) methanol-treated fibers.

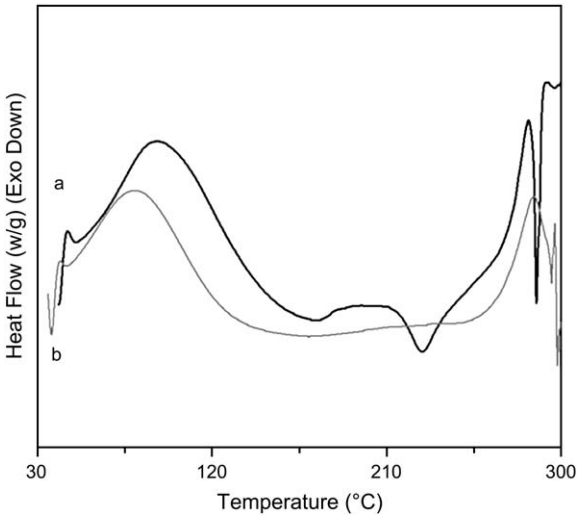

Fig. 7. DSC thermographs of fibers: (a) as-spun fibers, (b) methanol-treated fibers.

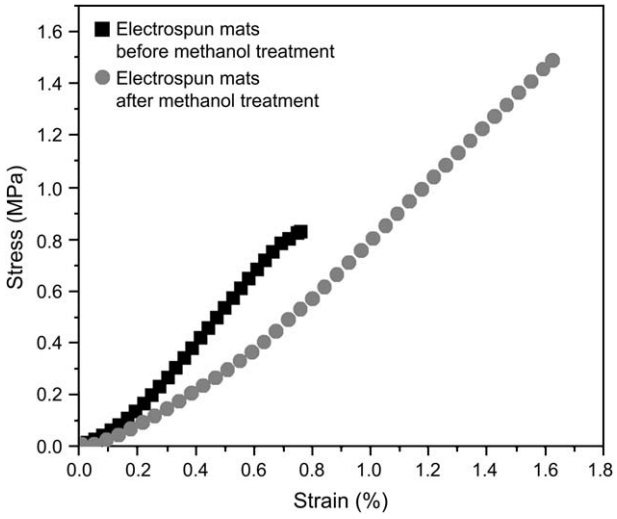

Fig. 8. Mechanical property plot of electrospun fibers.

3.4. Mechanical properties of the non-woven SF fibers

The results of the mechanical tests are shown in Fig. 8. As-spun fibers displayed a break stress of 0.82 MPa and strain of 0.76%, while after methanol treatment, with β-sheet structure formation, the stress and strain at break increased to 1.49 MPa and 1.63% respectively, which were comparable with the results obtained by Jin et al. [28] and Yang et al. [29]. The decrease in modulus of methanol-treated mats may be attributed to an increase in the flexibility; however, it is difficult to correlate these stress–strain curves with the structures in atomic level because the curves of these non-woven fibers depend on the assembles of these fibers rather than the structural character of a fiber molecule.

4. Conclusion

Electrospinning process of a stable aqueous solution at a high concentration was conducted successfully and the products were studied. The fibers had a belt-like morphology. The structure of as-spun fibers was predominantly random coil because there was not enough time for molecular arrangement and crystallization. As-spun mats had a break stress of 0.82 MPa and strain of 0.76%. After the traditional SF conformational transitions were induced with methanol, the stress and the strain at break increased to 1.49 MPa and 1.63%, respectively.

References

[1] Min BM, Lee G, Kim SH, Nam YS, Lee TS, Park WH. Biomaterials 2004;25:1289–97.
[2] Huang ZM, Zhang YZ, Kotakic M, Ramakrishna S. Composites Science and Technology 2003;63:2223–53.
[3] Ki CS, Baek DH, Gang KD, Lee KH, Um IC, Park YH. Polymer 2005;46:5094–102.
[4] Park WH, Jeong L, Yoo DI, Hudson S. Polymer 2004;45:7151–7.
[5] Gibson P, Schreuder-Gibson H, Rivin D. Colloids and Surfaces A 2001;187–188:469–81.
[6] Coffee RA. PCT/GB97/01968; 1998.
[7] Boland ED, Bowlin GL, Simpson DG, Wnek GE. Polymeric Materials, Science and Engineering Preprints 2001;85:51–2.
[8] Tretinnikov ON, Tamada Y. Langmuir 2001;17:7406–13.
[9] Andrew L. Materials Today 2004;7(2):21.
[10] Sukigara S, Gandhi M, Ayutsede J, Micklus M, Ko F. Polymer 2004;45:3701–8.
[11] Huang ZM, Zhang YZ, Ramakrishna S, Lim CT. Polymer 2004;45:5361–8.
[12] Min BM, Jeong L, Nam YS, Kim JM, Kim JY, Park WH. International Journal of Biological Macromolecules 2004;34:281–8.
[13] Zarkoob S, Reneker DH, Eby RK, Hudson SD, Ertley D, Adams WW. Polymer Preprints [American Chemical Society, Division of Polymer Chemistry] 1998;39:244–5.
[14] Ohgo K, Zhao CH, Kobayashi M, Asakura T. Polymer 2003;44:841–6.
[15] Kim SH, Nam YS, Lee TS, Park WH. Polymer Journal 2003;35:185–90.
[16] Wang M, Jin HJ, Kaplan DL, Rutledge GC. Macromolecules 2004;37:6856–64.
[17] Jin HJ, Fridrikh SV, Rutledge GC, Kaplan DL. Biomacromolecules 2002;3:1233–9.
[18] Lv Q, Cao CB, Zhai HZ, Zhu HS. Chinese Science Bulletin 2004;49:1009–11.
[19] Deitzel JM, Kleinmeyer J, Harris D, Tan NCB. Polymer 2001;42:261–72.
[20] Buchko CJ, Chen LC, Shen Y, Martin DC. Polymer 1999;40:7397–407.
[21] Koombhongse S, Liu WX, Reneker DH. Journal of Polymer Science Part B: Polymer Physics 2001;39:2598–606.
[22] Ayutsede J, Gandhi M, Sukigara S, Micklus M, Chen HE, Ko F. Polymer 2005;46:1625–34.
[23] Asakura T, Kuzuhara A, Tabeta R, Sait H. Macromolecules 1985;18:1841–5.
[24] Konishi T, Kondo M, Kurokawa M. Sen-i Gakkaishi 1967;23:64–9.
[25] Konishi T, Kurokawa M. Sen-i Gakkaishi 1968;24:550–4.
[26] Tusukada M. Journal of Sericulture Science of Japan 1986;55:126–30.
[27] Magoshi J, Magoshi Y, Nakamura S, Kasai N, Kakudo MJ. Journal of Polymer Science: Polymer Physics Edition 1977;15:1675.
[28] Jin HJ, Chen JS, Karageorgiou V, Altman GH, Kaplan DL. Biomaterials 2004;25:1039–47.
[29] Yang R, Fang P, Ko F. In: Kawabata S, Postle R, Niwa M, editors. Objective measurement: applications to product design and process control. Japan: The Textile Machinery Society of Japan; 1986. p. 547–56.